BNL-113459-2017-JA

High duty cycle Inverse Compton Scattering X-ray source

A. Ovodenko, R. Agustsson, M. Babzien, T. Campese, M. Fedurin, A. Murokh, I. Pogorelsky, M. Polyanskiy, J. Rosenzweig, Y. Sakai, C. Swinson, T. Shaftan

Submitted to Applied Physics Letters

January 2017

Collider-Accelerator Department

Brookhaven National Laboratory

U.S. Department of Energy
Office of Science,
Office of High Energy Physics

DISCLAIMER

High Duty Cycle Inverse Compton Scattering X-ray Source

A. Ovodenko[1], R. Agustsson[1], M. Babzien[2], T. Campese[1], M. Fedurin[2], A. Murokh[1a)], I. Pogorelsky[2], M. Polyanskiy[2], J. Rosenzweig[3], Y. Sakai[3], C. Swinson[2], and T. Shaftan[4]

[1] *RadiaBeam Technologies, LLC., 1717 Stewart St., Santa Monica, California, 90404, USA*
[2] *Accelerator Test Facility, Brookhaven National Laboratory, Upton, New York, 11973, USA*
[3] *University of California at Los Angeles, Los Angeles, California 90095, USA*
[4] *NSLS II, Brookhaven National Laboratory, Upton, New York, 11973, USA*

Abstract

Inverse Compton Scattering (ICS) is an emerging compact X-ray source technology, where small source size and high spectral brightness are of interest for multitude of applications. However, to satisfy practical flux requirements, a high-repetition-rate (multi-kHz) ICS system needs to be developed. To this end, this paper reports the experimental demonstration of a high peak brightness ICS source operating in a burst mode at 40 MHz. A pulse train interaction has been achieved by recirculating a picosecond CO_2 laser pulse inside an active optical cavity synchronized to the electron beam. The pulse train ICS performance has been characterized at 5- and 15- pulses per train and compared to a single pulse operation under the same operating conditions. With the observed near- linear X-ray photon yield gain due to recirculation, as well as noticeably higher operational reliability, the burst-mode ICS offers a great potential for practical scalability towards high duty cycles.

Inverse Compton Scattering (ICS) carries a promise of obtaining "synchrotron" quality, quasi-monochromatic, and directional X-ray light from a moderate-energy compact linacs [1,2]. In ICS, the high brightness X-ray outputs are attained via laser beam backscattered off relativistic electrons [3]. Similar to synchrotron light sources, ICS spectral coverage is achieved via relativistic Doppler shift, $k_x \sim k_l \gamma^2$, where k_x and k_l are wave numbers of the scattered X-ray and incoming laser beams, respectively, and γ is the Lorentz factor. However, in contrast to synchrotron light sources, the introduction of a micron-scale wavelength lasers in place of the centimeter-period undulators enables a dramatic reduction in size and cost of the system, and makes ICS an attractive technology to many applications in medicine [3,4], industry [5], research [6,7], and homeland security [8,9,10].

Recent experimental progress in characterization and optimization of single-shot ICS sources has been encouraging [11,12,13,14,15,16] and by combining a high-power laser with a low-emittance photocathode electron linac, ICS sources can attain *peak* brightness that exceeds that of the 3rd generation synchrotron light sources [14,17]. Indeed, the ICS peak and average brightness capabilities in the gamma range are unsurpassed by any other techniques [18,19,20,21]. However, a typical ICS output in a single laser/e-beam interaction is limited to about 10^7-10^8 photons in 1% bandwidth, and further efforts to enhance ICS flux by increasing laser intensity at the interaction point, are generally offset by the characteristic spectral broadening and energy outcoupling into harmonics [22]. Thus, in order to achieve the X-ray flux sufficient for practical applications a multi-pulse ICS system with about 10^3–10^4 interactions per second is sought.

The state-of-the-art normal conducting radio frequency photoinjectors typically operate at or below 100 Hz repetition rate [23], where conventional water-cooling techniques are sufficient in handling the microwave thermal dissipation in the injector. Thus, in order to achieve the desired 10^4 interactions per second, each macropulse must contain 100's of individual electron bunches interacting with the high peak power laser systems (> 100 mJ/pulse). In such a configuration, the ICS flux enhancement is achieved by a passive [24,25,26] or active [27] optical cavity operating in a burst mode, synchronized to electron beam pulse trains.

It is important to note that there is an alternative "continuous wave" (CW, as opposed to the above mentioned burst mode) approach, where a high finesse CW optical cavity [28] is incorporated into the CW electron beam source, i.e. storage ring [29,30] or an energy recovery linac [31,32]. Although CW systems have recently shown some success in a practical deployment [33], they also represent much more complex accelerator topologies. On the other hand, the burst mode regime provides the most direct path towards practical realization of the high flux ICS system, and is subject to the extensive ongoing investigation by multiple groups [34,35,36].

We report the experimental demonstration of the ICS flux enhancement in such an active recirculated configuration, performed at the Accelerator Test Facility (ATF) at Brookhaven National Laboratory (BNL). For this experiment, an active CO_2 laser optical cavity has been integrated into a beamline of the 60-MeV ATF linac that provides trains of picosecond, sub-nC electron bunches at the 24.5 ns period defined by the mode-locking frequency of a Nd:YAG laser used for a photocathode driver. The ICS interaction chamber has been integrated into a regenerative cavity of a CO_2 laser amplifier, as shown in FIG.

[a)] Authors to whom correspondence should be addressed. Electronic addresses: murokh@radiabeam.com

1(a). A seed CO_2 laser pulse (10.3 μm, 2 mJ, 4 ps) is produced by the front-end laser system that includes an optical parametric amplifier (OPA) and another CO_2 laser regenerative amplifier. The seed pulse is injected into the laser cavity by reflecting 4% of its energy along the cavity path by a NaCl window built into the cavity. A 4-atm CO_2 gas-discharge laser is utilized to amplify this low initial pulse energy to the sub-Joule level required for high-efficiency ICS and to maintain such pulses through multiple passes of the cavity. A pair of off-axis parabolic mirrors (OAP) focuses the laser beam at IP and re-telescopes for the next round-trip fitting it to the inter-electrode space of the laser amplifier (25 mm). These OAPs have central holes for the injecting and extracting the electron beam, and for extracting x-rays to the diagnostics placed at the end of the electron beam line.

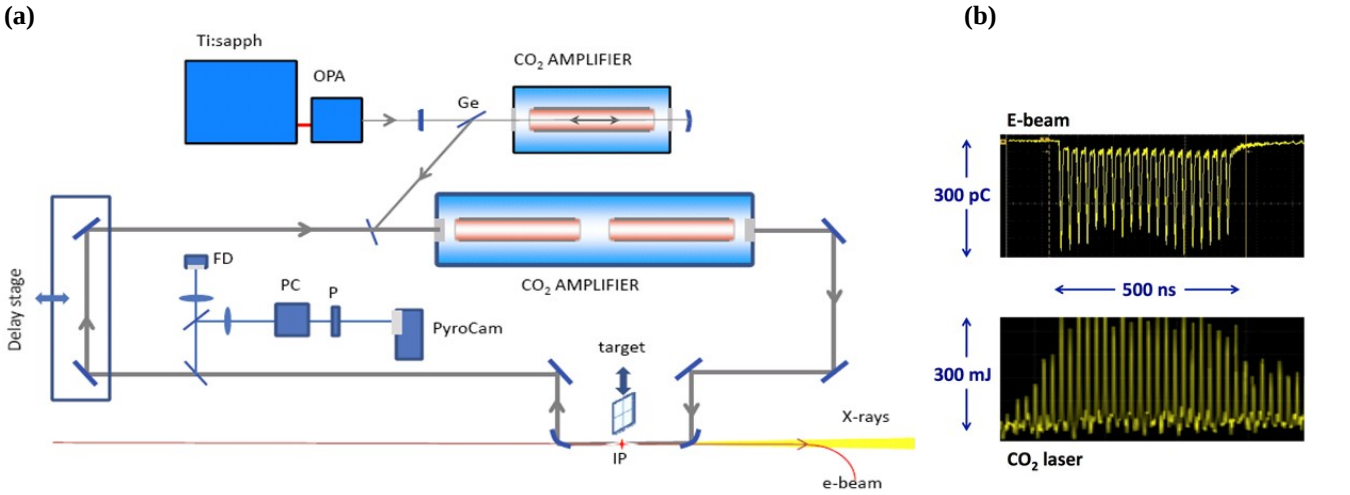

FIG. 1. (a) Principal optical diagram of the intracavity ICS experiment. Abbreviations: OPA – Optical Parametric Amplifier, IP – interaction point, P – polarizer, PC – Pockels Cell, FD – fast detector; (b) A scope trace for a train of 20 electron bunches separated by 24.5ns produced by linac and recorded by a strip-line before the ICS interaction chamber (top); a laser pulse train optimized for 20-bunch interaction, with a single pulse energy up to 350 mJ.

The optical cavity bench top commissioning results have been reported previously [27]; in these experiments we achieved generation of the laser pulse trains of up to 100 pulses at 40 MHz, with the average energy of 300 mJ per pulse. After the optical cavity was transferred to the electron beamline and re-commissioned, a laser train with about 30-40 pulses, with a combined total energy up to 8 J was established at the interaction point, to match the profile of the electron beam pulse train, shown in FIG. 1(b). The shot-to-shot laser pulse energy was measured using a calibrated joulemeter placed to intercept the reflection from a NaCl window. By fine-tuning the cavity optics and amplifier gain it was possible to alter and optimize the energy distribution inside the train.

Notably, the laser pulse trains' stability has been characterized not just by observing a reproducible pulse train envelope from shot-to-shot, but by ensuring the pointing stability of the laser focus at the IP. The laser beam at the IP was imaged onto a screen of an infrared camera (Spiricon PyroCam III). In order to discriminate each individual pass, the camera was placed behind crossed polarizers with a half-wave Pockels cell in between. By properly timing a 10-ns high-voltage pulse activating the Pockels cell, it was possible to verify the focal size and position of any individual laser pulse in the train. For the optimized beam, the observed position jitter was better than 25% of individual FWHM focal size measured at 190 μm. Initial synchronization between electron and laser pulses was obtained by adjusting the laser relative to the electron beam so that the separation between a signal from a fast detector on the laser beam path and the e-beam strip-line monitor was equal to the time-of-flight distance between them measured to the oscilloscope resolution (~1 ns). Finer timing was accomplished by measuring transmission of the laser through a thin germanium plate modulated by the electron-beam [37]. The synchronism between multiple pulses in the train is ensured by adjusting the length of the CO_2 laser's recirculating cavity with a delay stage, exactly equal to the length of the photocathode YAG cavity.

Compton X-rays produced by the laser/e-beam interaction propagate through the central hole of the OAP located downstream from IP and get extracted through a 250-μm-thick Be window, while the spent e-beam is deflected by a dipole magnet towards an in-vacuum beam-stop. The X-ray diagnostic station includes a calibrated Si detector used for absolute measurement of the X-ray yields and a micro-channel plate (MCP) for X-ray beam shape and position diagnostic. Given the ~8 mrad total divergence angle of the x-rays scattered by the 60 MeV electron beam and the 1.5 m distance of detectors from the source, we chose a Si detector (Canberra, A300) of the 25 mm diameter. To arrive at the detector, the X-ray beam propagates through 65 cm of air and a 250 μm beryllium window, resulting in an attenuation factor of ~5.1. In addition, a chevron type, 40 mm open area MCP (Photonis MCP 60:1 EDR KBR 6" FM P46) backed by a phosphor screen has been used for X-ray beam imaging.

For a 60 MeV electron beam, a single electron bunch interacting with a pulse from the plateau region of the CO_2 train produced a signal on a Si detector corresponding to the total photons yield of 2×10^7, which corresponds to an estimated

spectral brightness of about $7x10^5$ photons in 1% bandwidth per shot. This result was then used as a reference for MCP calibration, which was used to optimize the efficiency of multi-bunch shots. As shown in FIG. 2, a 5-bunch ICS interaction resulted in an increase in the total flux by a factor of 4.7 as compared to single bunch. The main parameters of the laser and electron beams used in the experiment, as well as of the observed x-ray signal are compiled in Table 1. The ICS photon cut-off energy 6.6 keV was verified through the use of the K-edge attenuation effect in Fe and Al metallic foils [38], acting as pre-calibrated low-pass and band-pass filters [22].

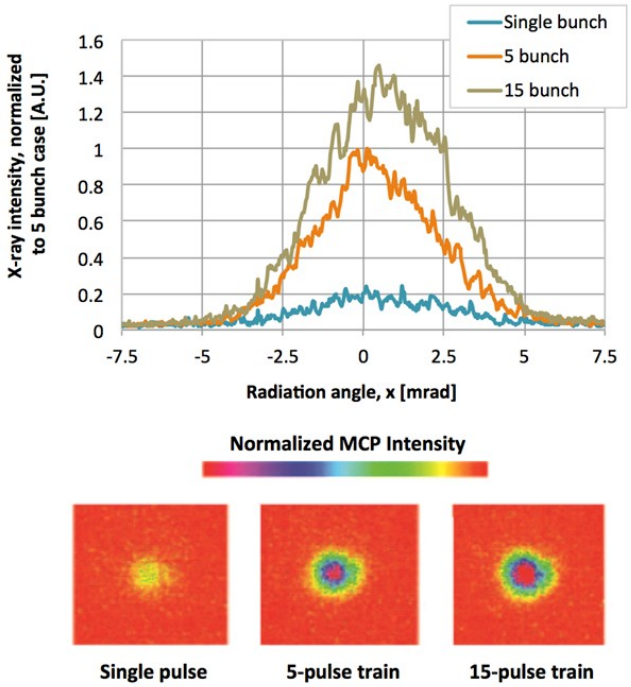

FIG. 2. Demonstration of the X-ray yield gain in a pulse train configuration. The images represent X-ray signals measured with the MCP, in a single pulse mode, and integrated over 5- and 15-pulse trains, respectively. An intensity profile above indicates near linear intensity gain from a single pulse to a 5-pulse train ICS, and about factor of 2 gain from 5-pulse to 15-pulse ICS.

The single shot yields in Table I is lower than those reported in prior single shot ICS experiments at ATF [22]. This is explained by a significantly reduced laser pulse energy, to enable multi-pass configuration (FIG. 1), and also a relatively relaxed spot sizes of the electron and laser beams, reducing by another order of magnitude the single-shot interaction efficiency. While the laser spot size was determined by a stable cavity mode, the electron beam could be focused to a much smaller spot using permanent magnet quadrupole (PMQ) triplets. The data reported in FIG. 2 were taken prior to PMQs installation; and when PMQs were installed for the final experimental run, the single shot ICS flux has increased 3-fold, as expected. However, the most consistent set of data reported herein was obtained prior to implementing the PMQ focusing.

Although the gain in cumulative x-ray yield from a single shot to 5-pulse train was nearly linear (FIG. 2), attempting to increase the number of interacting pulses from 5 to 15 resulted in only an additional factor of two X-ray flux gain. The deviation from linearity is best explained by degradation of the laser pulse upon amplification in the molecular gas active medium. Due to periodic spectral modulation the amplified rotational lines in the picosecond pulse result in splitting into a train of pulses. Such splitting, gradually developing over multiple passing of the pulse through the amplifier yields a spreading the laser pulse much beyond the Rayleigh range, thus, reducing the efficiency of the laser energy coupling with the electron bunch. This effect has been earlier observed and well characterized; in addition, a method for ameliorating this effect to it has been found [39]. The increase of the amplifier gas pressure and mixing of several CO_2 isotopes with admixed ^{18}O results in smoothing of the CO_2 amplifier gain spectrum sufficient for pulse-splitting mitigation. This approach will be implemented in the future CO_2 pulse train experiments.

TABLE I. Summary of the pulse-train ICS experimental parameters and results.

Electron Beam	
Spot size at IP, FWHM [μm]	180
Beam energy [MeV]	60
Charge per bunch [pC]	300
Bunch length, FWHM [ps]	6
Number of bunches	1-15
CO_2 Laser Pulse Train	
Waist size FWHM [μm]	190
Rayleigh range [mm]	8.8
Pulse energy [mJ]	300
Pulse length [ps]	5-150
Number of pulses	~20
Emitted X-Rays	
Photon energy [keV]	6.6
Radiation angle 1/γ [mrad]	8.5
Photon yield [single bunch]	2×10^7
Photon yield [5-pulse train]	10^8
Photon yield [15-pulse train]	2×10^8

Notably, the average X-ray flux was remarkably stable when compared to equivalent photon production in single-shot ICS systems, as is illustrated by three consecutive laser shots shown in FIG. 3. Partly, this enhanced reproducibility can be attributed to inherent laser's TEM00 mode stability in the well-aligned optical cavity, but mostly it reflects statistical advantages of a pulse-train interaction.

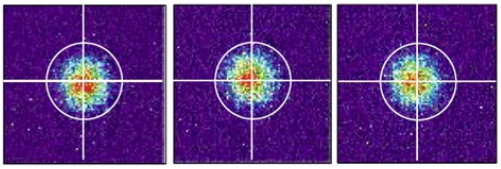

FIG. 3. Example of three consecutive shots in 5-bunch configuration exhibits an excellent stability of the x-ray source. The cross position is fixed on the MCP screen. A radius of the ring corresponds to 6-mrad angular divergence.

It is important to note that the observed deviation from linear growth for the 15-pulse train is not related to the electron beam multi-pulse effects, such as beam loading and beam break up (BBU) instability [40]. The beam loading induced energy spread was measured to be just over 1% across the pulse, and no visible emittance degradation has been observed in a pulse train mode. This is mostly due to the fact that there was a relatively low number of pulses, which at 40 MHz was insufficient to induce observable BBU effects that otherwise must be accounted in the design of longer pulse train and CW ICS sources [41,42]. Also, the same pulse train generation technique at BNL ATF was employed in previous experiments [24], and it was shown that a train of 20 pulses was focused to the 15 μm RMS spot size, ruling out a significant emittance degradation from BBU.

The results presented here conclusively demonstrate the X-ray flux gain in a multi-bunch ICS interaction scheme based an active laser cavity. The present design is shown to be capable of easily scaling the number of interacting pulses from one to fifteen, with the potential to reach even much higher multiplicative numbers upon optimization of the current experimental setup. In the case of the 5-pulse train, the total photon flux achieved was about $3\text{x}10^7$ photons in 1% bandwidth within 0.6 μs macropulse duration; which is few orders of magnitude higher flux intensity, than in other intra-cavity ICS experimental results reported to date [43 , 44]. It was also shown, that the pulse-train ICS has enhanced stability in shot-to-shot performance. These observations show that the pulse-train, burst mode solution used here represents a very promising approach to obtaining high average fluxes of ICS photons, a result which has high importance for future ICS projects worldwide.

This work is supported by DOE SBIR Grant No. DE-SC0007703, the US DOE contract DE-AC02-98CH10886, and US Dept. of Homeland Security Grant 2014-DN-077-ARI084-01.

1. P. Sprangle, A. Ting, E. Esarey, and A. Fisher, *J. Appl. Phys.* **72**, 5032 (1992).
2. E. Esarey, S. K. Ride, and P. Sprangle**,** *Phys. Rev. E* **48**, 3003 (1993).
3. F. E. Carroll, M. H. Mendenhall, R. H. Traeger, C. Brau, J. W. Waters, *Am. J Roentgenol*. **181**(5),1197 (2003).
4. P. Oliva, M. Carpinelli, B. Golosio, P. Delogu, M. Endrizzi, J. Park, I. Pogorelsky, V. Yakimenko, O. Williams and J. Rosenzweig, *Appl. Phys. Lett.* **97**, 134104 (2010).
5. D. F. Sunday, S. List, J. S. Chawla and R. J. Kline, *J. Appl. Cryst.* **48**, 1355 (2015).
6. D. J. Gibson, S. G. Anderson, C. P. J. Barty, S. M. Betts, R. Booth, W. J. Brown, J. K. Crane, R. R. Cross, D. N. Fittinghoff, F. V. Hartemann et al., *Phys. of Plasmas* **11**, 2857 (2004).
7. A. Bacci, I. Drebot, L. Serafini, V. Torri, V. Petrillo, E. Puppin, D. Alesini, M. Bellaveglia, F. Bisesto, B. Buonomo et al., in Proceedings of IPAC2016 Busan, Korea, 1747 (2016).
8. J. Pruet, D. P. McNabb, C. A. Hagmann, F. V. Hartemann and C. P. J. Barty, *J. Appl. Phys*. **99**, 123102-1-11 (2006).
9. J. Medalia, "Detection of Nuclear Weapons and Materials: Science,Technologies, Observations", CRS Report for Congress, Congressional Research Service 7-5700 R40154 pp. 12-13 (2008).
10. S. Boucher, P. Frigola, A. Murokh, I. Jovanovic, J. B. Rosenzweig, G. Travish, in Proceedings of PAC09, Vancouver, BC, Canada, 1387 (2009).
11. W. P. Leemans, R. W. Schoenlein, P. Volfbeyn, A. H. Chin, T. E. Glover, P. Balling, M. Zolotorev, K. J. Kim, S. Chattopadhyay, and C. V. Shank, Phys. Rev. Lett. **77**, 4182 (1996).
12. M. Babzien, I. Ben-Zvi, K. Kusche, I. V. Pavlishin, I. V. Pogorelsky, D. P. Siddons, V. Yakimenko, D. Cline, F. Zhou, T. Hirose et al., *Phys. Rev. Lett.* **96**, 054802 (2006).
13. V. Yakimenko and I. V. Pogorelsky, *Phys. Rev. ST Accel. Beams* **9**, 091001 (2006).
14. F. Albert, S. G. Anderson, D. J. Gibson, C. A. Hagmann, M. S. Johnson, M. Messerly, V. Semenov, M. Y. Shverdin, B. Rusnak, A. M. Tremaine et al., *Phys. Rev. ST Accel. Beams* **13**, 070704 (2010).
15. J. B. Rosenzweig and O. Williams, *Inter. J. Modern Phys. A* **23**, 4333 (2007)
16. F. H. O'Shea, O. Williams, G. Andonian, S. Barber, Y. Sakai, J. B. Rosenzweig, I. Pogorelsky, M. Fedurin, K. Kusche, and V. Yakimenko*, Phys. Rev. ST Accel. Beams* **15**, 020702 (2012)
17. I.V. Pogorelsky, I. Ben-Zvi, T. Hirose, S. Kashiwagi, V. Yakimenko, K. Kusche, P. Siddons, J. Skaritka, T. Kumita, A. Tsunemi et al., Phys. Rev. ST Accel. Beams **3**, 090702 (2000).
18. ELI-NP Gamma Beam System (the ELI-NP Compton Source) ELI-NP-GBS Technical Design Report, See http://arxiv.org/abs/1407.3669, (2014).
19. F. V. Hartemann, W. J. Brown, D. J. Gibson, S. G. Anderson, A. M. Tremaine, P. T. Springer, A. J. Wootton, E. P. Hartouni, and C. P. J. Barty, *Phys. Rev. ST Accel. Beams* **8**, 100702 (2005)
20. R. Hajima, T. Hayakawa, N. Kikuzawa and E. Minehara, *J. of Nucl. Sci. and Tech.* **45** (5), 441-451 (2008).
21. C. P. J. Barty, *SPIE Opt. Optoelectron*. Paper 8080B-30 (2011).
22. Y. Sakai, I. Pogorelsky, O. Williams, F. O'Shea, S. Barber, I. Gadjev, J. Duris, P. Musumeci, M. Fedurin, A. Korostyshevsky et al., *Phys. Rev. ST Accel. Beams* **18**, 060702 (2015).
23. L. Faillace, R. Agustsson, P. Frigola, A. Verma, H. Badakov, A. Fukasawa, J. Rosenzweig, A. Yakub, F. Cianciosi, P. Craievich and M. Trovo, in Proceedings of IPAC2013, Shanghai, China, 2905 (2013).
24. A. Murokh, R. Agustsson, S. Boucher, P. Frigola, T. Hodgetts, A. Ovodenko, M. Ruelas, R. Tikhoplav, M. Babzien, M. Fedurin et al., in Proceedings of IPAC2012, New Orleans, LA, 3245-3248 (2012).
25. I. Jovanovic, M. Shverdin, D. Gibson, C. Brown, *Nucl. Instr. and Meth*. *A* **578**, 160 (2007).
26. K. Dupraz, K. Cassou, N. Delerue, P. Fichot, A. Martens, A. Stocchi, A. Variola, F. Zomer, A. Courjaud, E. Mottay et al., *Phys. Rev. ST Accel. Beams*, **17**, 033501 (2014).
27. I. Pogorelsky, R. Agustsson, T. Campese, A. Murokh, A. Ovodenko, M. Polyanskiy and T. Shaftan, *J. Phys. B: At. Mol. Opt. Phys.* **47**, 234014 (2014).
28. T. Akagi, S. Araki, Y. Funahashi, Y. Honda, H. Kataoka, T. Kon, S. Miyoshi, T. Okugi, T. Omori, K. Sakaue et al., *Nucl. Instr. and Meth*. *A* **724**, 63 (2013).
29. Z. Huang, R. D. Ruth, "Laser Electron Storage Ring*", Phys. Rev. Letters* **80** (5), 976-979 (1998).
30. C. Bruni, Y. Fedala, J. Haissinski, M. Lacroix, B. Mouton, R. Roux, A. Variola, G. Wormser, F. Zomer, P. Brunelle *et al*., *AIP Conf. Proc.* **1228**, 68 (2010).
31. T. Hirose, K. Dobashi, Y. Kurihara, T. Muto, T. Omori, T. Okugi, I. Sakai, J. Urakawa, M. Washio, *Nucl. Instr. and Meth*. *A* **455**, 15 (2000).
32. "Report of the Basic Energy Sciences Workshop on Compact Light Sources", See http://science.energy.gov/~/media/bes/pdf/reports/files/CLS.pdf (2010).
33. K. Achterhold, M. Bech, S. Schleede, G. Potdevin, R. Ruth, R. Loewen and F. Pfeiffer, *Nat. Sci. Rep.* **3**,1313 (2013).
34. A. Murokh, "Compact high brightness sources of tunable X-rays", presented at SPIE Photonics West 2016, (2016).
35. W. S. Graves, J. Bessuille, P. Brown, S. Carbajo, V. Dolgashev, K.-H. Hong, E. Ihloff, B. Khaykovich, H. Lin, K. Murari et al., *Phys. Rev. ST Accel. Beams*, **17**, 120701 (2014).
36. B. van der Geer, "Smart*Light: The Dutch X-Band-based Compact Compton Back-scattering Source", presented at OSA Workshop on High-Brightness Sources and Light-Driven Interactions, Long Beach, CA (2016).
37. P. B. Corkum, A. J. Alcock, and K. E. Leopold, *J. Appl. Phys*. **50**, 3079 (1979).

38. O. Williams, G. Andonian, M. Babzien, E. Hemsing, K. Kusche, J. Park, I. Pogorelsky, G. Priebe, J. Rosenzweig, V. Yakimenko, *Nucl. Instr. and Meth*. *A* **608**, S18 (2009).
39. M. N. Polyanskiy, I. V. Pogorelsky, V. Yakimenko, *Opt. Express* **19**, 7717 **(**2011).

40. F. J. Sacherer, “Tranverse Bunched Beam Instabilities – Theory”, in Proceeding of High Energy Accelerator, 347 (1974).
41. A. Bacci, D. Alesini, P. Antici, M. Bellaveglia, R. Boni, E. Chiadroni, A. Cianchi, C. Curatolo, G. Di Pirro, A. Esposito et al., *J. Appl. Phys*. **113**, 194508 (2013)
42. G. H. Hoffstaetter and I. V. Bazarov, *Phys. Rev. ST Accel. Beams* **7**, 054401 (2004).
43. K. Sakaue, M. Washio, S. Araki, M. Fukuda, Y. Higashi, Y. Honda, T. Omori, T. Taniguchi, N. Terunuma, J. Urakawa and N. Sasao, *Rev. Sci. Instrum.* **80**, 123304 (2009).
44. H. Shimizu, M. Akemotoa, Y. Araia, S. Arakia, A. Arysheva, M. Fukudaa, S. Fukudaa, J. Habaa, K. Haraa, H. Hayanoa et al., *Nucl. Instr. and Meth*. *A* **772**, 26 (2015).